Author(s): Savin, H. & Kuivalainen, P. & Lebedeva, N. & Novikov, S.

Title: Spin disorder scattering in a ferromagnetic insulator-on-graphene structure

Year: 2013

Version: Post print

Please cite the original version:

Savin, H. & Kuivalainen, P. & Lebedeva, N. & Novikov, S.. 2013. Spin disorder scattering in a ferromagnetic insulator-on-graphene structure. Physica Status Solidi B. Volume 251, Issue 2. 407-414. DOI: 10.1002/pssb.201350024.

Spin disorder scattering in a ferromagnetic insulator-on-graphene structure

H. Savin, P. Kuivalainen*, N. Lebedeva, and S. Novikov

Department of Micro and Nanosciences, School of Electrical Engineering, Aalto University, P.O. Box 13500, FI-00076 Aalto, Finland

Keywords graphene, quantum transport, critical scattering, magnetic semiconductor

*Corresponding author: e-mail pekka.kuivalainen@aalto.fi

We theoretically study the transport properties of a single graphene layer between two insulating materials, i.e., a ferromagnetic EuO thin film and a nonmagnetic SiC substrate. An exchange interaction between the charge carrier spins in graphene and the localized magnetic moments in the ferromagnetic insulator is assumed. This proximity effect and the large spin fluctuations at temperatures close to the ferromagnetic transition temperature T_C lead to spin disorder scattering, which is calculated using a Green's function technique. Numerical results indicate that at temperatures close to T_C the contribution of the spin disorder scattering to the total electron mobility is clearly observable even in the case of a weak exchange interaction and a low background mobility of the graphene layer. This enables the experimental determination of the exchange interaction parameter using the present model and a simple resistivity measurement.

1 Introduction

Graphene, an atomically thin layer of carbon atoms arranged in a honeycomb lattice, continues to attract enormous interest because of its unusual physical properties as well as due to its applications in carbon based electronics [1-5]. A number of peculiar transport phenomena, such as finite minimal conductivity [2], the unusual half-integer quantum Hall effect [6], and Klein paradox [7] have been studied in graphene. In graphene-based electronics [5] the high carrier mobility [8, 9] is one of the most attracting properties. Due to the small spin–orbit coupling [10], weak hyperfine interaction with the underlying nuclear spin system, and potentially long spin lifetimes graphene also is a promising material for spintronic applications (see, e.g., Ref. [11] and refs. therein). Spin relaxation lengths on the order of micrometers have been observed [12] together with spin relaxation times of hundreds of picoseconds. Also spin injection from ferromagnetic Co into graphene has been achieved [13]. Recently highly efficient spin transport in epitaxial graphene on SiC has been reported showing spin transport efficiencies up to 75% and spin diffusion lengths exceeding 100 μm [14]. Several approaches for controlling the spin-dependent transport in graphene nanostructures have been proposed. For instance, graphene quantum dots have been identified as an ideal host for spin qubits [15, 16]. Also the spin polarized states induced by the edge defects in zigzag graphene nanoribbons have been studied in a number of works [17-20], and it has been predicted theoretically that graphene nanomesh structure should show magnetic properties [21].

An alternative approach to graphene-based spintronics has been proposed by Semenov et al. [22] and Haugen et al. [23], who theoretically studied spin dependent transport properties of graphene having a ferromagnetic insulator deposited on top of the graphene layer. Here the spin manipulation

is achieved via the exchange interaction between the spins of the itinerant electrons in graphene and the spins of the localized magnetic electrons in the magnetic atoms at the surface of the ferromagnetic insulator. Also the possibility to control the spin dependent electrical current using a ferromagnetic gate has been discussed in several works [24-28]. Due to the spin splitting of the electronic states a spin polarized current is generated, and it can be controlled by the gate voltage. A drawback in these structures is that due to the lack of the energy band gap, the spin polarization in a 2D monolayer graphene is limited [24-26]. The situation is more favorable in bilayer graphene due to its specific electronic structure, as discussed by Semenov et al. [28] and Hung Nguyen et al. [29]. Strong resonant tunneling effects and large magnetoresistance behavior have been predicted [29, 30] in the case of the ferromagnetic insulator/bilayer graphene-structures. So far the exact value of the strength of the exchange interaction in the graphene/ferromagnetic insulator-interface is unknown, but in the EuO/Al-interface an estimate of $J_{exch} = 15$ meV has been obtained experimentally [31]. This value would be large enough to cause, e.g., a significant spin splitting of the electronic states in graphene [23]. Recently even a much larger value for the exchange parameter in an EuO/graphene-system was estimated based on first-principle calculations [32].

In the present paper, we theoretically study the effect of the proximity exchange interaction and the consequent spin disorder scattering on the electrical transport in a single layer graphene between two insulating layers, i.e., a nonmagnetic SiC substrate and the ferromagnetic EuO thin film on top of the graphene layer. The spin disorder scattering has not been treated in the previous works [22-30] on ferromagnetic graphene. Our aim is to show that since graphene has a very high electron mobility, which is very sensitive to external perturbations, the effect of the proximity exchange coupling could easily be seen in the measurements of the electron mobility versus temperature and magnetic field. In this way also an estimate for the exchange coupling parameter J_{exch} could be obtained, which is the key parameter in all the modeling of the graphene-based spintronic devices utilizing the proximity effect. The EuO/graphene/SiC-structure was chosen as a model system, because EuO is an ideal isotropic ferromagnetic insulator, the magnetic properties of which are well known. Furthermore, the fabrication of ferromagnetic EuO thin films on graphene has been demonstrated recently [33, 34]. The advantage of the SiC substrate is that an existence of a band gap has been reported in the graphene/SiC system [35]. Later the results of Zsou et al. [35] have been questioned by other groups [36-38]. However, there are alternative proposals for insulating substrates or nanostructures, which also should induce a band gap in graphene, such as hexagonal boron nitride (h-BN) [39], graphene nanomesh [40], hydrogenated h-BN [41], and nanoperforated graphene [42]. Therefore, our assumption of a band gap in graphene is reasonable. Finally, the existence of the band gap is not critical for the spin disorder scattering, since strong spin disorder scattering is observed in ferromagnetic metals having no band gap [43-45]. We have chosen the model system with a band gap, since the band gap and the existence of ordinary charge carriers with a finite effective mass make the calculations of the mobility more straightforward.

Originally the theory of the spin disorder scattering, also known as critical scattering, was developed for ferromagnetic metals by de Gennes and Friedel [43], later by Fisher and Langer [44], and more recently by Majumbar and Littlewood [45]. The spin disorder scattering in magnetic semiconductors was discussed first by Haas [46], and later the mobility model was improved by Sinkkonen [47], who estimated the relaxation time of the charge carriers from the imaginary part of the self-energy in the self-consistent Born approximation. Also the transport anomalies observed in diluted magnetic semiconductors typically have been explained using various versions of the theory of spin disorder scattering [48-54]. In the present work, we estimate the spin disorder scattering rate from the second order self-energy, which is calculated using a Green's function technique in the case of a proximity exchange interaction between the spins of the itinerant electrons in graphene

and the spins of the localized magnetic electrons of the magnetic Eu atoms in EuO at the EuO/graphene interface.

2 Model and formulation

We study the ferromagnetic graphene system shown in Fig. 1. The epitaxial single layer graphene layer (denoted by C–C in Fig. 1) is sandwiched between an insulating non-magnetic substrate such as SiC and a ferromagnetic insulator (FMI), which we assume to be a EuO thin film. The gate metal (G) on top of the FMI layer is optional, i.e., it will not be considered further in the present work, but it is important if the structure of Fig. 1 is used in a transistor-like operation. We start the presentation of the model by reviewing briefly the standard "massless Dirac-fermion" model [55, 56], and then we add to it the effects of the insulating substrate and the ferromagnetic EuO layer as perturbations.

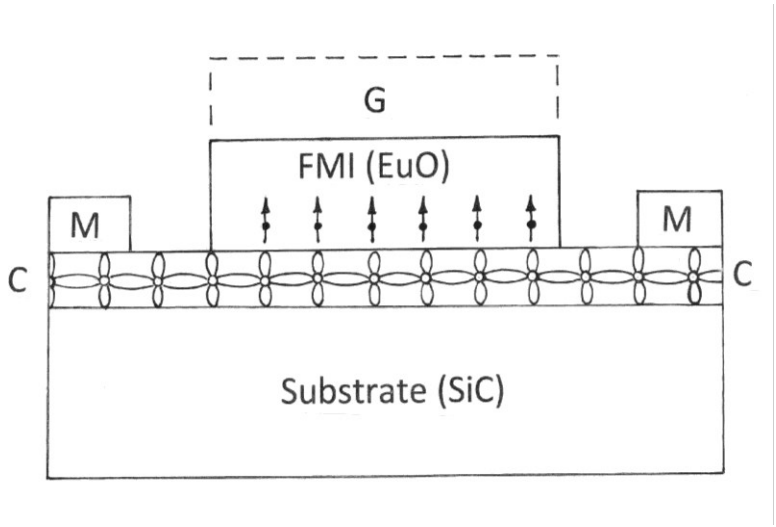

Figure 1. Schematic drawing of a ferromagnetic graphene structure, where a 2D graphene layer (C–C) is between an insulating substrate (SiC) and a EuO thin film, which is a ferromagnetic insulator (FMI). The electrical transport occurs in the graphene layer between two nonmagnetic contacts (M). The carrier concentration in the graphene layer can be controlled by adding a gate metal (G) to the system.

The honeycomb lattice of graphene has two carbon atoms per unit cell on sites, denoted below by *A* and *B*. The energy bands relevant to charge transport are formed from the sp^2 orbitals. The mobile charge carriers move in the *x*–*y* plane by hopping between the p_z orbitals of the carbon atoms. The low energy band structure consists of Dirac cones located at the two inequivalent Brillouin zone corners *K* and *K′*. The Hamiltonians for these valleys are given by

$$H_K^0 = \hbar \qquad \hbar \begin{pmatrix} 0 & k_x - ik_y \\ \kappa_x + \imath\kappa_y & 0 \end{pmatrix} \quad (1)$$

$$H_{K'}^0 = \hbar \qquad \hbar \begin{pmatrix} 0 & k_x + ik_y \\ \kappa_x - \imath\kappa_y & 0 \end{pmatrix} \quad (2)$$

where v_F is the Fermi velocity and the Pauli matrices $\boldsymbol{\sigma}$ act on the sublattice degrees of freedom. For each wave vector $\boldsymbol{k}$, Eq. (1) has two eigenstates [55]:

$$\psi_{\mathbf{ks}}(\mathbf{r},\pm) = \frac{1}{\sqrt{2}}\left(\langle \mathbf{r}|\mathbf{k},A\rangle e^{-i\theta_{\mathbf{k}}/2} \pm \langle \mathbf{r}|\mathbf{k},B\rangle e^{i\theta_{\mathbf{k}}/2}\right)|\chi_{\mathbf{s}}\rangle$$

$$= \frac{1}{\sqrt{2S_{area}}}\left(e^{i\mathbf{k}\cdot\mathbf{r}}e^{-i\theta_{\mathbf{k}}/2} \pm e^{i\mathbf{k}\cdot\mathbf{r}}e^{i\theta_{\mathbf{k}}/2}\right)|\chi_{\mathbf{s}}\rangle \quad (3)$$

where $|\chi_s\rangle$ is the carrier spin eigenstate, $\boldsymbol{s}$ is the spin operator of a carrier, S_{area} is the area of the graphene surface, and $\theta_k = \arctan(k_y/k_x)$. The eigenenergies of the Hamiltonian (1) are given by

$$E_k^0 = \pm\hbar \quad (4)$$

which shows that there is no band gap between the valence and conduction bands in a single layer graphene. The calculation of the Green's function for the graphene below requires the presentation of the Hamiltonians in the second quantization formalism. Therefore, using the wave functions (3), we define the following field operators for the charge carriers in graphene:

$$\Psi(\mathbf{r}) = \sum_{\mathbf{k},\mathbf{s}} \psi_{\mathbf{ks}}(\mathbf{r}) c_{\mathbf{ks}} \quad (5)$$

$$\Psi^{\dagger}(\mathbf{r}) = \sum_{\mathbf{k},\mathbf{s}} \psi^{*}_{\mathbf{ks}}(\mathbf{r}) c^{\dagger}_{\mathbf{ks}} \quad (6)$$

where $c^{\dagger}_{ks}(c_{ks})$ is the creation (annihilation) operator of the charge carrier in the state $|\boldsymbol{k}\rangle|\chi_s\rangle$.

Next we add the effects of the perturbations due to the substrate (SiC) and the ferromagnetic insulator (EuO) to the electronic structure described above. Zhou et al. [35] have shown that in an epitaxial graphene on a SiC substrate a band gap $E_g \approx 0.26\,\text{eV}$ is induced by the breaking of the A and B sublattice symmetry owing to the graphene–substrate interaction. Then the eigenstates can be obtained by diagonalization the Hamiltonian $H = H_K^0 + H'$ including (1) (or (2)) and a perturbation H', which simply is given by

$$H' = \begin{pmatrix} \frac{E_g}{2} & 0 \\ 0 & -\frac{E_g}{2} \end{pmatrix} \quad (7)$$

The perturbation caused by the exchange interaction is more complicated. Let us consider a ferromagnetic insulator in a close contact with a single graphene layer so that there is an overlap between the p_z-orbitals of graphene and the localized wave functions of the magnetic electrons on the magnetic atoms at the FMI/graphene-interface. In the case of EuO there are seven 4f-electrons in each Eu-atom, which are responsible for the ferromagnetic properties of EuO and which give rise to the total spin $S = 7/2$ per Eu-atom. Then the Hamiltonian for the exchange interaction between the itinerant electrons in graphene and the magnetic electrons in FMI is given by

$$H_{exch} = H^0_{exch} + V_{exch} = -\sum_{\mathbf{R}} J(\mathbf{r}-\mathbf{R})\mathbf{s}\cdot\langle \mathbf{S}_{\mathbf{R}}\rangle - \sum_{\mathbf{R}} J(\mathbf{r}-\mathbf{R})\mathbf{s}\cdot\left(\mathbf{S}_{\mathbf{R}} - \langle \mathbf{S}_{\mathbf{R}}\rangle\right) \quad (8)$$

where the summation runs over the 2D lattice sites $\boldsymbol{R}$ in the FMI/graphene-interface, and $J(\boldsymbol{r}-\boldsymbol{R})$ is the exchange interaction potential, which depends on the overlap of the wave functions. $\boldsymbol{S}_R$ is the spin operator for the total spin of the magnetic atom at the site $\boldsymbol{R}$. We have divided the Hamiltonian (8) into a mean-field part H^0_{exch}, which is proportional to the average spin polarization of the magnetic atoms, $\langle \boldsymbol{S}_R \rangle$, and a fluctuation part V_{exch}, which is depends on $(\boldsymbol{S}_R - \langle \boldsymbol{S}_R \rangle)$. The former is responsible for the spin polarization of the electronic states and the latter causes the spin disorder scattering [43-47]. We assume that the exchange potential is of the contact type and it is given by

$$J(\mathbf{r}-\mathbf{R}) = \Omega_U J_{exch}\delta(\mathbf{r}-\mathbf{R}) \quad (9)$$

Here $\Omega_U = S_{\mathrm{area}}/N$, and N is the number of the Eu atoms at the interface, J_{exch} is the exchange interaction parameter, and $\delta(\boldsymbol{r}-\boldsymbol{R})$is Dirac's δ-function. Using the field operators (5) and (6) and the exchange potential (9) we can express the exchange interaction (8) in the second quantization form:

$$\hat{H}_{exch} = \int d^3\mathbf{r}\Psi^{\dagger}(\mathbf{r})H_{exch}(\mathbf{r})\Psi(\mathbf{r}) = \hat{H}^0_{exch} + \hat{V}_{exch} \quad (10)$$

with

$$\hat{H}^0_{exch} = -\frac{\Delta_{exch}}{2}\sum_{\mathbf{k}}\left(c^{\dagger}_{\mathbf{k}\uparrow}c_{\mathbf{k}\uparrow} - c^{\dagger}_{\mathbf{k}\downarrow}c_{\mathbf{k}\downarrow}\right) \quad (11)$$

and

$$\hat{V}_{exch} = \sum_{\substack{\mathbf{R},\mathbf{k},\mathbf{k}'\\ \mathbf{s},\mathbf{s}'}} \langle \psi_{\mathbf{ks}} | J(\mathbf{r}-\mathbf{R})\mathbf{s} | \psi_{\mathbf{k's'}}\rangle \cdot \left(\mathbf{S}_{\mathbf{R}} - \langle \mathbf{S}_{\mathbf{R}}\rangle\right) c^{\dagger}_{\mathbf{ks}}c_{\mathbf{k's'}} \quad (12)$$

The Hamiltonian (11) describes the giant Zeeman splitting of the electronic states with

$$\Delta_{exch} = J_{exch}\langle S^z \rangle \quad (13)$$

where $\langle S^z \rangle$is the average spin–polarization of the ferromagnetic lattice in the FMI layer. The effect of the exchange interaction (11) on the electronic structure of the EuO/graphene/SiC system shown in Fig. 1 is obtained by finding the eigenvalues for the following Hamiltonian:

$$H^{tot}_K = H^0_K + H' + H^0_{exch}$$

$$= \hbar \begin{pmatrix} \frac{E_g}{2} - \frac{\Delta_{exch}}{2}\left(\delta_{s\uparrow} - \delta_{s\downarrow}\right) & -k_x + ik_y \\ -k_x + ik_y & -\frac{E_g}{2} - \frac{\Delta_{exch}}{2}\left(\delta_{s\uparrow} - \delta_{s\downarrow}\right) \end{pmatrix} \quad (14)$$

which was obtained by adding the exchange interaction to the combination of the Hamiltonians (1) and (7). By diagonalizing the matrix (14) we get the spin polarized eigenenergies, which are given by

$$E_{\mathbf{ks}} = -\frac{\Delta_{exch}}{2}\left(\delta_{s\uparrow} - \delta_{s\downarrow}\right) \pm \sqrt{\left(\frac{E_g}{2}\right)^2 + (\hbar \quad \quad \quad} \quad (15)$$

Here the sign +(−) refers to the conduction (valence) band. The low energy region of the energy band structure is shown in Fig. 2, as calculated from Eq. (15). At small values of the wave vector, $|\boldsymbol{k}| \ll E_g/2\hbar v_F$, the band structure resembles the one in the ordinary magnetic semiconductors having a parabolic wave vector-dependence, $E_{\boldsymbol{k}} \propto |\boldsymbol{k}|^2$.

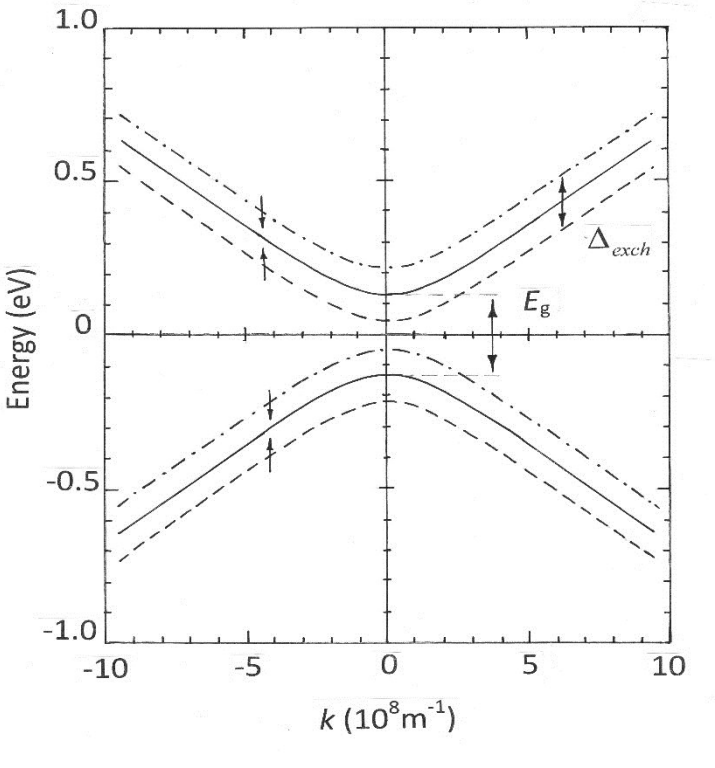

Fig.2. Low energy spectrum of energy bands in a EuO/graphene/SiC structure of Fig. 1. The material parameters are $J_{exch} = 0.05$ eV, $S = 7/2$, $E_g = 0.26$ eV [30], and $v_F = 10^6$ m s^{-1}. The solid curves show the spin degenerate bands ($\Delta_{exch} = 0$), and the dashed (dash-dotted) curves show the spin-up (spin-down) bands, when $\Delta_{exch} = J_{exch}S$.

The Green's function $\hat{G} = (E - \hat{H}_0 - \hat{V}_{exch})^{-1}$ for the electrons in the graphene layer is calculated using the operator (12) as a perturbation. Then the unperturbed Hamiltonian includes the spin polarized bands (15), and it is given by

$$\hat{H}_0 = \sum_{\mathbf{ks}} E_{\mathbf{ks}} c_{\mathbf{ks}}^{\dagger} c_{\mathbf{ks}} \quad (16)$$

Now the corresponding unperturbed Hamiltonian is given by $\hat{G}0 = (E - \hat{H}_0)^{-1}$. Following our previous treatments [50, 51] of the spin-dependent transport in magnetic semiconductors in the case of the weak exchange interaction, it is a straightforward task to solve the proper equation of motion for the Green's function $\hat{G}$, and the solution is given by

$$G(E, E_{\mathbf{ks}}) = \left[E - E_{\mathbf{ks}} - \Sigma_{exch}^{(2)}(E_{\mathbf{ks}}) \right]^{-1} \quad (17)$$

where the second order self-energy related to the exchange interaction (12) reads

$$\Sigma_{exch}^{(2)}(\mathbf{k}s; E) = \frac{J_{exch}^2}{N} \sum_{\mathbf{q}} \left(\frac{C^{xx}(q)\delta_{s\uparrow}}{E - E_{\mathbf{k-q},\downarrow}} + \frac{C^{yy}(q)\delta_{s\downarrow}}{E - E_{\mathbf{k-q},\uparrow}} + \frac{C^{zz}(q)}{E - E_{\mathbf{k-q}}} \right) \quad (18)$$

Here $C^{\alpha\alpha}(q)'$s with $\alpha\alpha = xx$, yy, or zz, are the three components of the Fourier transform of the spin correlation function [47] $C(R, R') = \langle (\boldsymbol{S}_R - \langle \boldsymbol{S}_R \rangle) \cdot (\boldsymbol{S}_{R'} - \langle \boldsymbol{S}_{R'} \rangle) \rangle$, and they are given by

$$C^{\alpha\alpha}(\mathbf{q}) = \frac{C_o(T)}{\kappa_{\alpha\alpha}^2 + a_0^2 q^2} \quad (19)$$

where

$$C_0(T) = \frac{S^2(S+1)T}{T_C} \quad (20)$$

and

$$\kappa_{xx}^2 = \kappa_{yy}^2 = 3\left\{ \frac{(S+1)T}{S\left[B_S(y)/y \right] T_C} - 1 \right\} \quad (21)$$

$$\kappa_{zz}^2 = 3\left\{ \frac{(S+1)T}{S\left[\partial B_S(y)/\partial y \right] T_C} - 1 \right\} \quad (22)$$

Here a_0 is the lattice constant of EuO, and $B_S(y)$ is the Brillouin function with the argument y, which is related to the average molecular field acting on the spin $\boldsymbol{S}_R$. The Brillouin function describes well the magnetic properties of EuO, which are close to those of an ideal ferromagnet.

The electron mobility μ_{SD}^{s} limited by the spin disorder scattering is calculated using the standard relation $\mu_{SD}^{s} = e\tau_{k_F s}/m^*$, where the inverse of the effective mass $(m^*)^{-1}$ is calculated from the second derivative of the energy E_{ks} in Eq. (15), and the average relaxation time $\tau_{k_F s}$ at the Fermi level E_F is calculated from the imaginary part of the self-energy (18). At low temperatures in the case of the 2D electron gas in graphene we get

$$\frac{1}{\tau_{\mathbf{k}_F s}} = \frac{2\left|\mathrm{Im}\,\Sigma^{(2)}_{exch}(E_{\mathbf{k}_F s})\right|}{\hbar} = \frac{J^2_{exch}\Omega_U}{8\pi^2\hbar}\int_0^{2\pi} d\varphi \int_0^{\infty} dq q \left\{ \frac{C^{xx}\left(\sqrt{k_{Fs}^2+q^2-k_{Fs}q\cos\varphi}\right)\gamma\delta_{s\uparrow}}{\gamma^2+\left(E_{\mathbf{k}_F s}-E_{\mathbf{q}\downarrow}\right)^2} \right.$$

$$\left. + \frac{C^{yy}\left(\sqrt{k_{Fs}^2+q^2-k_{Fs}q\cos\varphi}\right)\gamma\delta_{s\downarrow}}{\gamma^2+\left(E_{\mathbf{k}_F s}-E_{\mathbf{q}\uparrow}\right)^2} + \frac{C^{zz}\left(\sqrt{k_{Fs}^2+q^2-k_{Fs}q\cos\varphi}\right)\gamma}{\gamma^2+\left(E_{\mathbf{k}_F s}-E_{\mathbf{q}s}\right)^2} - \right\} \quad (23)$$

Here γ is a small parameter describing the collisional broadening effects [51], and at small values of γ the function $\gamma/(\gamma^2+x^2)\pi$ in Eq. (23) approaches the delta-function $\delta(x)$. The value of the relaxation time (23) depends on the spin index $s(=\uparrow \text{ or } \downarrow)$. The contributions from the spin-up and spin down bands (see Fig. 2) to the mobility are added together as follows

$$\mu_{SD} = \frac{\mu^{\uparrow}_{SD} n_{\uparrow} + \mu^{\downarrow}_{SD} n_{\downarrow}}{n_{\uparrow}+n_{\downarrow}} \quad (24)$$

where $n_{\uparrow(\downarrow)}$ is the electron concentration in the spin-up (spin-down) subband, when the total carrier concentration is $n = n_{\uparrow} + n_{\downarrow}$.

In our transport model the other scattering mechanisms are taken into account using a phenomenological expression for the background mobility μ_{BG} without spin disorder scattering, and it is given by

$$\mu_{BG}(T) = \mu_{RT}\left(\frac{T}{300K}\right)^{-\beta} \quad (25)$$

Here μ_{RT} is the room temperature mobility in graphene, when the spin disorder scattering is neglected. Typically in graphene resistivity decreases and mobility increases with decreasing temperature [9, 57-60], which can be modeled using Eq. (25) with $\beta \geq 1$ the parameter . Finally, the total mobility $\mu^{-1}_{TOT} = \mu^{-1}_{SD} + \mu^{-1}_{BG}$ μ_{TOT} can be calculated using Eqs. (24) and (25) and Mathiessen's rule,.

3 Numerical results and discussion

We have calculated the electrical transport properties of the EuO/graphene/SiC structure shown in Fig. 1 using the model presented above. The most important material parameters in our model are the exchange interaction constant J_{exch} in Eqs. (15) and (23) and the room temperature mobility μ_{RT} in Eq. (25). Unfortunately experimental data for J_{exch} in the case of the EuO/graphene interface is not yet available, but based on the experimental results for a EuO/Al system a value $J_{exch} = 0.015$ eV has been estimated previously [23]. In the case of other FMI's even higher values, such as $J_{exch} = 0.065$ eV, have been suggested [28]. Recently a theoretical estimation for the exchange interaction induced spin splitting $\Delta_{exch} = 36\,\mathrm{meV}$ was presented for the EuO/graphene system [32]. However, all the estimated values are much smaller than the experimental value $J_{exch} = 0.17$ eV for bulk EuO samples [61]. Due to the lack of information about the exact value of J_{exch} we calculate the spin disorder scattering limited mobility in the cases of weak ($J_{exch} = 0.005$ eV) and intermediate ($J_{exch} = 0.05$ eV) couplings. The values of electron mobility in nonmagnetic graphene also vary a lot from sample to sample [9, 58, 59], typically in the range from 10^3 to 10^5 cm^2 V^{-1} s^{-1}, depending on

the quality of the graphene layer and on its interaction with other materials in contact with graphene. In our calculations we let the room temperature mobility vary from 10^2 to 10^4 cm^2 V^{-1} s^{-1} in order to see how much the background mobility masks the effect of the spin disorder scattering. The other material parameters used in the calculations are the following: Curie temperature $T_C = 70$ K in EuO thin films [62], $a_0 = 5.14$ Å (EuO), $S = 7/2$, $v_F = 10^6$ m s^{-1}, $E_g = 0.26$ eV (graphene), $\gamma = 10$ meV, and $\beta = 1$.

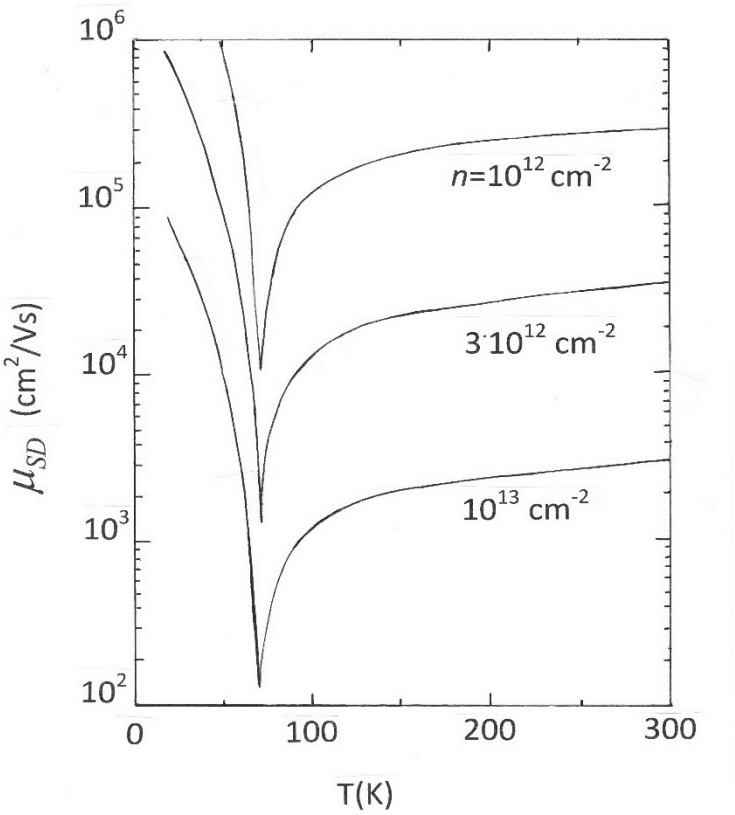

Figure 3. Spin disorder scattering limited mobility μ_{SD} versus temperature for various electron concentrations in graphene. Here the value of the exchange interaction parameter is $J_{exch} = 0.05$ eV.

Figure 3 shows the calculated mobility μ_{SD} versus temperature for various electron concentrations in the EuO/graphene/SiC structure of Fig. 1. There is a sharp minimum in mobility at $T = T_C$, which is similar to the one in ordinary ferromagnetic semiconductors [50]. This is caused by the spin fluctuations in the magnetic lattice of EuO, which are largest at the Curie temperature: According to Eq. (23), the inverse of the relaxation time (and mobility) is proportional to the Fourier transform of the spin correlation functions (19), which at small values of the wave vector $|\boldsymbol{q}|$ diverge at $T = T_C$ as $1/|T - T_C|$. The mobility μ_{SD} in Fig. 3 decreases with increasing electron concentration, because at larger Fermi wave vectors the integrand in Eq. (23) increases. Also the effective mass, as calculated from the second derivative of the dispersion relation (15), $m^{*-1} \propto \mathrm{d}^2E(k)/\mathrm{d}k^2$, increases with increasing carrier concentration.

Figure 4 shows the mobility μ_{SD} versus temperature at various magnetic fields, when the electron concentration in graphene is 3×10^{12} cm^{-2}. Two different values for the exchange interaction parameter J_{exch} were used. The large negative magnetoresistance is shown at temperatures close to T_C. At temperatures below T_C the temperature dependence of mobility is much weaker in the case of

the small coupling constant $J_{exch} = 0.005$ eV (the four uppermost curves in Fig. 4) than in the case of the larger constant $J_{exch} = 0.05$ eV (the four lowest curves). This is due to the smaller spin splitting Δ in the case of small J_{exch}, which means that then the both subbands are occupied and the both spin correlation functions C^{zz} and C^{xx} (or C^{yy}) in Eq. (23) contribute to the mobility.

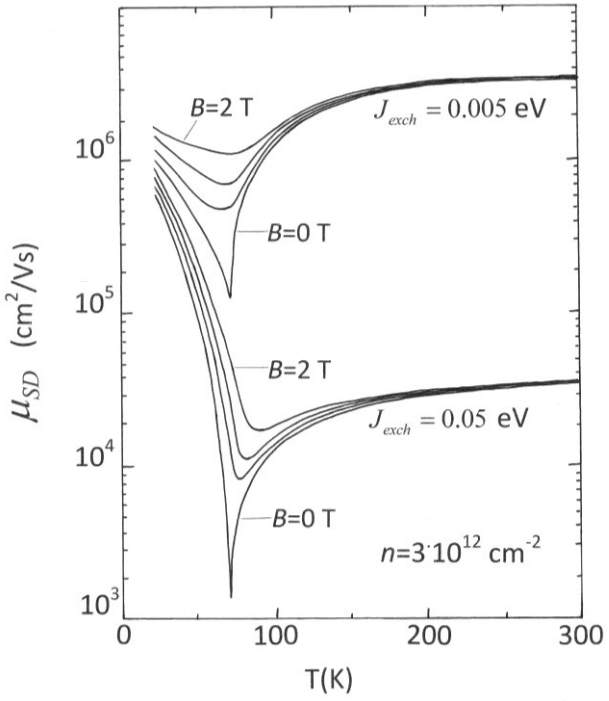

Figure 4. Spin disorder scattering limited mobility μ_{SD} versus temperature at various magnetic fields. In the upper (lower) curves the exchange interaction parameter is $J_{exch} = 0.005$ eV (0.05 eV). The charge carrier concentration in graphene is $3 \times 10^{12}\,\mathrm{cm}^{-2}$. The other material parameters are the same as in Fig. 3. The external magnetic field values are 0, 0.5, 1, and 2 T from bottom to top in the both cases of the two J_{exch} values.

In the case of the larger spin splitting only the spin down subband is occupied, $n_{\downarrow} \approx 0$, and scattering events between the subbands are rare. Then the mobility depends only on C^{zz}, which depends more strongly on temperature at $T < T_C$ than C^{xx} and C^{yy}.

Figure 5 shows the calculated resistivity $\rho = (en\mu_{TOT})^{-1}$ versus temperature, when the external magnetic field is either $B = 0$ T or $B = 1$ T and the carrier concentration in graphene is 10^{13} cm^{-2}. The room temperature mobility varies from 10^2 to 10^4 cm^2 V^{-1} s^{-1}. Figure 5 shows that even in the case of low background mobility $\mu_{BG}(300\,\mathrm{K}) = \mu_{RT} = 100\,\mathrm{cm}^2\,\mathrm{V}^{-1}\,\mathrm{s}^{-1}$, and an intermediate exchange coupling between EuO and graphene, $J_{exch} = 0.05$ eV, a sharp peak in resistivity appears at the Curie temperature, when the external magnetic field is zero.

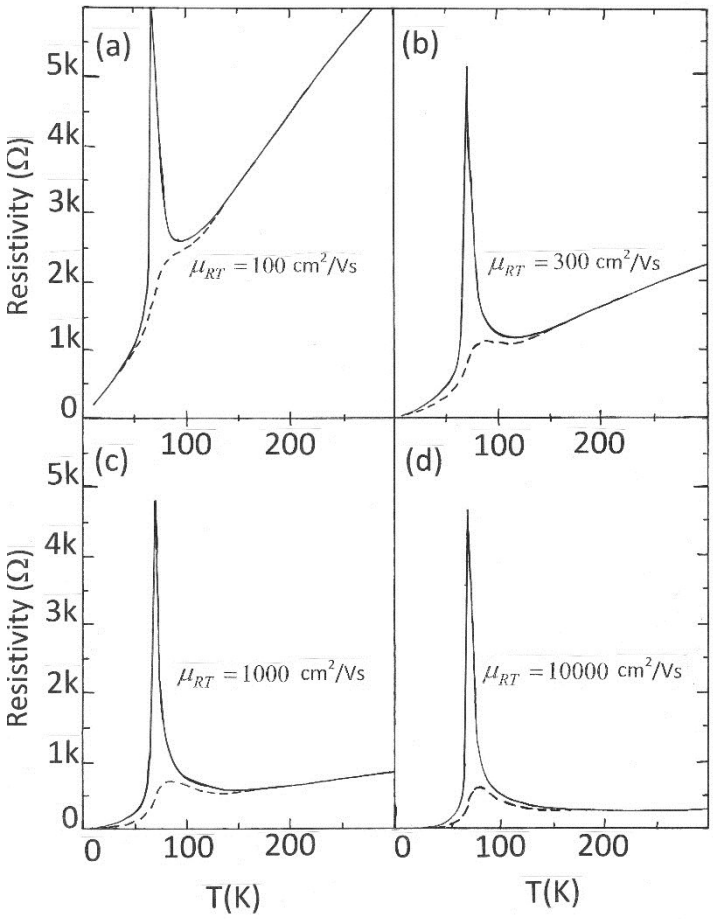

Figure 5. Calculated resistivity versus temperature at two values of the external magnetic field, $B = 0$ T (solid curves) and $B = 1$ T (dashed curves), when the carrier concentration is 10^{13} cm^{-2}, and the exchange interaction parameter $J_{exch} = 0.05$ eV. The background mobility at room temperature is (a) 100 cm^2 V^{-1} s^{-1}, (b) 300 cm^2 V^{-1} s^{-1}, (c) 10^3 cm^2 V^{-1} s^{-1}, and (d) 10^4 cm^2 V^{-1} s^{-1}.

An interesting question is, whether the resistivity peak can be observed also in the case of the weak exchange coupling. Figure 6a shows that the contribution from the spin disorder scattering is barely observable in the ρ versus T-curve, when the coupling constant is reduced to the value 0.005 eV. However, when the derivative of ρ with respect to temperature is calculated as a function of temperature there is a prominent peak at $T = T_C$, which then disappears when the external magnetic field is increased from 0 to 1 T. Therefore we believe that in simple resistivity and magnetoresistance measurements the contribution from the spin disorder scattering could be observed experimentally in the EuO/graphene/SiC structure even in the case of the low electron mobility and the weak proximity effect. Thereby also an experimental estimate for the exchange interaction parameter J_{exch} could be obtained.

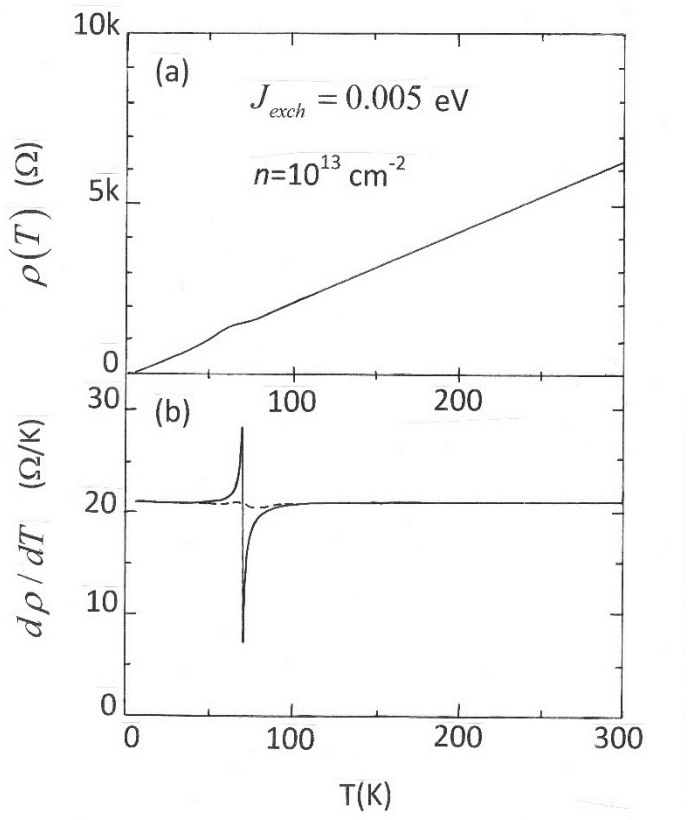

Figure 6. (a) Resistivity versus temperature at $B = 0$ T in the case of the weak coupling constant $J_{\text{exch}} = 0.005$ eV and the low background mobility $\mu_{\text{RT}} = 100$ cm^2 V^{-1} s^{-1}. The electron concentration is $n = 10^{13}$ cm^{-2}. (b) Derivative of the resistivity with respect to temperature as a function of temperature at $B = 0$ T. The dashed curve has been calculated at $B = 1$ T.

4 Conclusions

We have calculated the contribution from the spin disorder scattering to the temperature and magnetic field dependent electron mobility and resistivity in a ferromagnetic insulator-on-graphene system. We have shown that even in the case of a weak exchange interaction between the itinerant electrons in graphene and the localized magnetic electrons in EuO, a resistivity peak and negative magnetoresistance at the Curie temperature of EuO could be observable experimentally in simple resistivity measurements. Our calculations indicate that due to its specific temperature and magnetic field dependences the contribution from the spin disorder scattering should be detectable also in the case of graphene having poor quality and, consequently, a low electron mobility. Fitting our model to the measured resistivity and magnetoresistance as a function of temperature, an estimate for the strength of the proximity effect between graphene and EuO could be obtained. The model can be extended to the cases of other ferromagnetic insulators having Curie temperatures higher than EuO, which could pave the way to the room temperature spintronics in graphene-based device structures.

Acknowledgement

This work has been supported by the Academy of Finland.

References

[1] K. S. Novoselov, A. K. Geim, S. V. Morozov, D. Jiang, Y. Zang, S. V. Dubonos, I. V. Grigorieva, and A. A. Firsov, Science 306, 666 (2004).

[2] K. S. Novoselov, A. K. Geim, S. V. Morozov, D. Jiang, M. I. Katsnelson, I. V. Grigorieva, S. V.

Duborius, and A. A. Firsov, Nature (London) 438, 197 (2005).

[3] A. K. Geim and K. S. Novoselov, Nature Mater. 6, 183 (2007).

[4] M. C. Lemme, T. J. Echtermeyer, M. Baus, and H. Kurz, IEEE Electron Device Lett. 28, 282 (2007).

[5] F. Schwierz, Nature Nanotechnol. 5, 487 (2010).

[6] Y. Zhang, Y. W. Tan, H. L. Stormer, and P. Kim, Nature (London) 438, 201 (2005).

[7] M. I. Katsnelson, K. S. Novoselov, and A. K. Geim, Nature Phys. 2, 620 (2006).

[8] S. V. Morozov, K. S. Novoselov, M. I. Katsnelson, F. Schedin, D. C. Elias, J. A. Jaszczak, and A. K. Geim, Phys. Rev. Lett.100, 016602 (2008).

[9] K. I. Bolotin, K. J. Sikes, J. Hone, H. L. Stormer, and P. Kim, Phys. Rev. Lett. 101, 096802 (2008).

[10] C. L. Kane and E. J. Mele, Phys. Rev. Lett. 95, 226801 (2005).

[11] O. V. Yazyev, Rep. Prog. Phys. 73, 056501 (2010).

[12] N. Tombros, C. Jozsa, M. Popinciuc, H. T. Jonkman, and B. J. van Wees, Nature 448, 571 (2007).

[13] W. Han, K. Pi, K. M. McCreary, Y. Li, J. J. I. Wang, A. G. Swartz, and R. K. Kawakami, Phys. Rev. Lett. 105, 167202 (2010).

[14] B. Dlubak, M.-B. Martin, C. Deranlot, B. Servet, S. Xavier, R. Mattana, M. Sprinkle, C. Berger, W. A. De Heer, F. Petroff,A. Anane, P. Senor, and A. Fert, Nature Phys. 8, 557 (2012).

[15] B. Trauzettel, D. V. Bulaev, D. Loss, and G. Burkard, Nature Phys. 3, 192 (2007).

[16] P. Recher and B. Trauzettel, Nanotechnology 21, 302001 (2010).

[17] Y.-W. Son, M. L. Cohen, and S. G. Louie, Nature (London) 444, 347 (2006).

[18] M. Wimmer, I. Adagideli, S. Berber, D. Tomanek, and K. Richter, Phys. Rev. Lett. 100, 177207 (2008).

[19] W. Y. Kim and K. S. Kim, Nature Nanotechnol. 3, 408 (2008). [20] F. Munos-Rojas, J. Fernandez-Rossier, and J. J. Palacios, Phys. Rev. Lett. 102, 136810 (2009).

[21] H.-X. Yang, M. Chshiev, D. W. Boukhvalov, X. Waintal, and S. Roche, Phys. Rev. B 84, 214404 (2011).

[22] Y. G. Semenov, K. W. Kim, and J. M. Zavada, Appl. Phys. Lett. 91, 153105 (2007).

[23] H. Haugen, D. Huertas-Hernando, and A. Brataas, Phys. Rev. B 77, 115406 (2008).

[24] T. Yokoyama, Phys. Rev. B 77, 073413 (2008).

[25] V. Dam Do, V. Hung Nguyen, P. Dollfus, and A. Bournel, J. Appl. Phys. 104, 063708 (2008).

[26] J. Zou, G. Jin, and Y.-Q. Ma, J. Phys.: Condens. Matter 21, 126001 (2009).

[27] V. Hung Nguyen, V. Nam Do, A. Bournel, V. Lien Nguyen, and P. Dollfus, J. Appl. Phys. 106,

053710 (2009).

[28] Y. G. Semenov, J. M. Zavada, and K. W. Kim, Phys. Rev. B 77, 235415 (2008).

[29] V. Hung Nguyen, A. Bournel, and P. Dollfus, Appl. Phys.Lett. 95, 232115 (2009).

[30] V. Hung Nguyen, A. Bournel, and P. Dollfus, J. Appl. Phys. 109, 073717 (2011).

[31] G. M. Roesler, M. E. Filipkowski, P. R. Broussard, Y. U. Idzerda, M. S. Osofsky, and R. J. Soulen, in: Superconducting Superlattices and Multilayers, Vol. 2157, edited by I. Bozovic (Proc. SPIE, Los Angeles, CA, 1994), pp. 285–290.

[32] H.-X. Yang, A. Hallal, D. Terrade, X. Waintal, S. Roche, and M. Chshiev, Phys. Rev. Lett. 110, 046603 (2013).

[33] A. G. Swartz, P. M. Odenthal, Y. Hao, R. S. Ruoff, and R. K. Kawakami, ACS Nano 6, 10063 (2012).

[34] D. F. Förster, T. O. Wehling, S. Schumacher, A. Rosch, and T. Michely, New J. Phys. 14, 023022 (2012).

[35] S. Y. Zhou, G.-H. Gweon, A. V. Fedorov, P. N. First, W. A. De Haar, D.-H. Lee, F. Guinea, A. H. CastroNeto, and A. Lanzara, Nature Mater. 6, 770 (2007).

[36] E. Rotenberg, A. Bostwick, T. Ohta, J. L. McChesney, T. Seyller, and K. Horn, Nature Mater. 7, 258 (2008).

[37] C.-H. Park, F. Giustino, C. D. Spataru, M. L. Cohen, and S. G. Louie, Nano Lett. 9, 4234 (2009).

[38] G.-Z. Kang, D.-S. Zhang, and J. Li, Phys. Rev. B 88, 045113 (2013).

[39] G. Giovannenetti, P. A. Khomyakov, G. Brocks, P. J. Kelly, and J. van den Brink, Phys. Rev. B 76, 073103 (2007).

[40] J. Bai, X. Zhong, S. Jiang, Y. Huang, and X. Duan, Nature Nanotechnol. 5, 190 (2010).

[41] N. Kharche and S. K. Nayak, Nano Lett. 11, 5274 (2011). [42] M. Kim, N. S. Safron, E. Han, M. S. Arnold, and P. Gopalan, Nano Lett. 10, 1125 (2010).

[43] P. G. de Gennes and J. Friedel, J. Phys. Chem. Solids 4, 71 (1958).

[44] M. E. Fisher and J. S. Langer, Phys. Rev. Lett. 20, 665 (1968).

[45] P. Majumdar and P. B. Littlewood, Nature 395, 479 (1998).

[46] C. Haas, Phys. Rev. 168, 531 (1968).

[47] J. Sinkkonen, Phys. Rev. B 19, 6407 (1979).

[48] A. Van Esch, L. Van Bockstal, J. De Boeck, G. Verbanck, A. S. van Steenbergen, P. J. Wellmann, B. Grietens, R. Bogaerts, F. Herlack, and G. Borghs, Phys. Rev. B 56, 13103 (1997).

[49] F. Matsukura, H. Ohno, A. Shen, and Y. Sugawara, Phys.Rev. B 57, R2037 (1998).

[50] P. Kuivalainen, Phys. Status Solidi B 227, 449 (2001).

[51] P. Kuivalainen and N. Lebedeva, Phys. Status Solidi B 231, 512 (2002).

[52] E. H. Hwang and S. Das Sarma, Phys. Rev. B 72, 035210 (2005).

[53] V. Novak, K. Olejnik, J. Wunderlich, M. Cukr, K. Vyborny, A. W. Rushforth, K. W. Edmonds, R. P. Campion, B. L. Gallagher, J. Sinova, and T. Jungwirth, Phys. Rev. Lett. 101, 077201 (2008).

[54] T. Dietl, J. Phys. Soc. Jpn. 77, 031005 (2008).

[55] T. Ando, J. Phys. Soc. Jpn. 74, 777 (2005).

[56] D. P. DiVincenzo and E. J. Mele, Phys. Rev. B 29, 1685 (1984).

[57] E. H. Hwang and S. Das Sarma, Phys. Rev. B 77, 115449 (2008).

[58] J. L. Tedesco, B. L. VanMil, R. L. Myers-Ward, J. M. McCrate, S. A. Kitt, P. M. Campbell, G.

G. Jernigan, J. C. Culbertson, C. R. Eddy, and D. K. Garskill, Jr., Appl. Phys. Lett. 95, 122102 (2009).

[59] X. Hong, A. Posadas, K. Zon, C. H. Ahn, and J. Zhu, Phys. Rev. Lett. 102, 136808 (2009).

[60] E. V. Castro, H. Ochoa, M. I. Katsnelson, R. V. Gorbachev, D. C. Elias, K. S. Novoselov, A. K. Geim, and F. Guinea, Phys. Rev. Lett. 105, 266601 (2010).

[61] P. G. Steeneken, L. H. Tjeng, I. Elfimov, G. A. Sawatzky, G. Ghiringhelli, N. B. Brookes, and D. J. Huang, Phys. Rev. Lett. 88, 047201 (2002).

[62] T. S. Santos and J. S. Moodera, Phys. Rev. B 69, 241202(R) (2004).